3-D Mold Fabrication for Polymer Replication: Experimentation and Optimization

Chung-Soo Kim[1] and Jeong-Bin Park[1]

1 School of Mechanical and Aerospace Engineering, Seoul National University, building 301, Room 1405, San 56-1, Shinlim-Dong, Kwanak-gu, Seoul, South Korea, 123-456

KEYWORDS : Focused ion beam, sputtering, spiral scan, micro/nano-scale mold, design of experiment, Taguchi method

Focused ion beam sputtering has a potential for fabricating mold-making applications below in micro/nano-scale. This mold is capable of engaging the mass production of micro/nanoscale components by embossing, injection molding, and other replica methods. As reported previously from Vasile (pixel dwell time control) and Fu (2-D slice by slice approach), the challenge lies in making arbitrary shapes such as curved or non-linear shape. This work involves only experimental results by making the modification of 2-D slice by slice approach by converting discrete to continuous process with the combination of the spiral scan. So as to fabricate the conical shape mold on the silicon substrate, several types of FIB-concerned parameter and fabrication tragedy were defined and designed, and Taguchi's method for robust design also is applied for specific evaluation form. In consequence, by using nanoscale measurement tool such as SEM, SIM, and AFM, the structural stability (diameter, depth, sidewall angle) and efficiency (sputter yield, cost) were evaluated, and also related physical phenomena was observed. Finally, microscale mold having conical shape was manufactured the circular cone on PUA and PDMS.

Manuscript received: August 27, 2002 / Accepted: April 30, 2003

1. Introduction

Focused ion beam (FIB) technology is widely used for a numerous applications including failure analysis, magnetic head trimming, device prototyping, and transmission electron microscopy (TEM) sample preparation by providing various advantages of fabricating micro/nanoscale structures [1-3]. There are many methods for making micro-mold such as charged particle lithography, deep reactive ion etching (RIE), etc. for micro-lenses, fluidic channels, and any functional patterns [4-6]. Among these methods, the FIB-milling can give a capability to develop various sizes of micro/nano molds and stamps through replication method like embossing, injection molding, and any lithography [5,7-9]. This mold-making for replication gives a great potential for mass production. However, there are not much of studies on fabricating 3-dimension structures like arbitrary structure, especially in curved structures. As reported previously, two types of schematics are presented for fabricating the curved structure by both Vasile *et al.* (1997-2006) [8-10] and Fu *et al.*[11]. Vasile *et al.* introduced depth control method by controlling the pixel dwell time, and Fu *et al.* improved by two-dimensional slicing, which is much simplified mathematically the Vasile's method.

In this study, we applied the spiral scan method, which is reported as a good method for circular pattern [12], in a part of vector scan. To fabricate the 3-D mold having conic structure, the modified fabrication method of Fu *et al.* was introduced by repeating the ion beam scans to whole discrete slices approximately thousand-times.

In order to fabricate the sub-microscale conical structure on silicon for polymer replication, the two types of fabrication parameter, including the ion beam and process parameter, were carefully investigated. Moreover, the effect of four critical parameter, when ion beam sputtering, of the processing parameter of ion dose (count number), dwell time, overlap, and slice number are determined and experimented by using design of experiment, adopting orthogonal array.

The full 3-D silicon micro-mold was fabricated though the orthogonal array by investigating effective parameters, and measured its dimension by nanoscale instrumentation such as scanning electron microscopy (SEM), scanning ion microscopy (SIM) and atomic force microscopy (AFM). By setting the feature definition for evaluation, the experimental result was evaluated by Taguchi's method. The optimum condition for structural stability and efficiency was resulted, and some physical phenomena were discussed further.

2. Nanofabrication by FIB

In order to fabricate the micro mold, the commercial FIB system (SMI 3050: SII Nanotechnology) was used. Its ion source consists of liquid gallium, and it can provide the energy up to 30 KeV. In this FIB system, there exist two types of parameters which are a beam and processing parameter, and scan method such as raster, serpentine, and vector scan method. In case of beam parameter, ion energy, ion current, spot diameter, and current density are included. For processing parameter, ion dose, dwell time, beam overlap, and pixel size, which vary by field of view (FOV), and refresh time. In this article, the vector scan method was applied so as ion beam to make a circular cone shape. Next section will illustrate in detail other conditions.

2.1 Scan method

There are not much of experimental studies of vector scan, but the spiral scan as a part of vector scan gave a good result for circular hole,

compared to the raster scan. Therefore, the spiral scan was applied to fabricate the silicon micro-mold. The difference and the schematics of both the raster and vector scan are shown in Fig. 1.

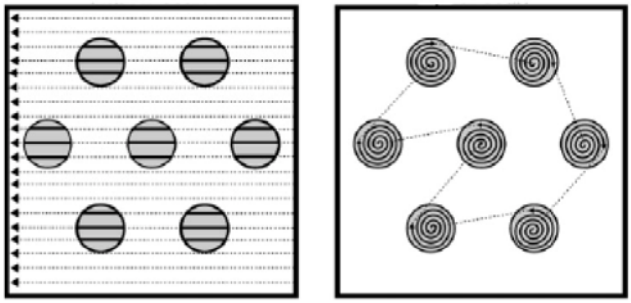

(a) (b)

Fig. 1 Raster (a) and vector (b) scan routine.

2.2 Continuous slicing method

In case of Fu *et al*., they fabricated the curved structure by using 2-D slice by slice approach when FIB sputtering. Moreover, each slice was fabricated discretely like step by step. In here, we make a difference by fabricating the each slice continuously, as explained in Fig. 2. As seen in Fig. 2, the number of slice is added as a parameter for FIB processing. For this approach, the ion dose must be converted to count number, which indicates that how many scans can be applied to each slice. For example, if 100 counts are applied for 8 numbers of slices, 800 scans are applied for one structure in consequence. Thus, this count number directly determines the ion dose.

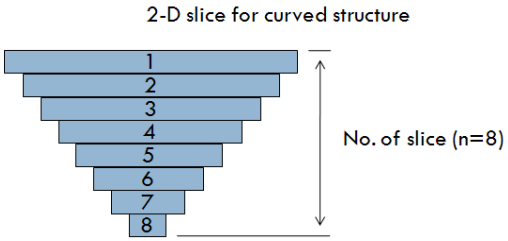

Fig. 2 Schematics of slice by slice approach: discrete approach (one process from 1 to 8) and continuous approach (repeat process from 1 to 8).

2.2 Parameter selection

For the sake of making 1 μm scale circular cone, the 30 KeV of Ga2+ ion beam, 91 pA of ion current, 30 nm of spot diameter, and 12.924 of current density were selected at a specific FOV of 24 um scale which can directly define the pixel size of 30 nm. In here, both spot size and pixel size are the same value. It explains that the ion beam is controlled pixel by pixel.

After selecting the ion beam condition, the prerequisite experiment was performed. As a result, the circular cone with 1.2 um in a diameter having a depth of 760 nm at the condition of 20000 total count, 1 μsec dwell time, 100 % overlap, and 10 numbers of slice, as shown in Fig. 3.

Furthermore, other processing parameter, including No. of slice for design of experiment were determined in Table 1. Furthermore, the total count is related to the number of slice because the total count is divided by the number of slice. For example, when the total count and the number of slice are 100 and 10 respectively, the ion beam scans 10 times for 1 slice.

Based on above prerequisite experiment, the experimental condition was determined as in Table 1, and experiments were performed according to orthogonal array in Table 2. Through these 9 experiments, the 3-D micro-mold structure was constructed as shown in Fig.4. The fabricated structure was measured by atomic force microscope (AFM).

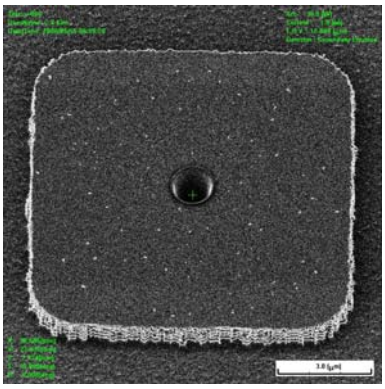

Fig. 3 FIB fabricated circular cone with dimension of 1.2 μm diameter having 760 nm: Fabrication condition is 20000 total count, 1 μsec dwell time, 100 % overlap, and 10 numbers of slice.

Table 1 The level of factors

Level	Factor			
	Total count	Dwell time	Overlap	No. of slice
1	10000	0.5	0.5	5
2	20000	1	1	10
3	30000	2	1.5	15

Table 2 Orthogonal array

Exp. No	Factor			
	Total count (unit)	Dwell time (unit)	Overlap	No. of slice
1	1	1	1	1
2	1	2	2	2
3	1	3	3	3
4	2	1	2	3
5	2	2	3	1
6	2	3	1	2
7	3	1	3	2
8	3	2	1	3
9	3	3	2	1

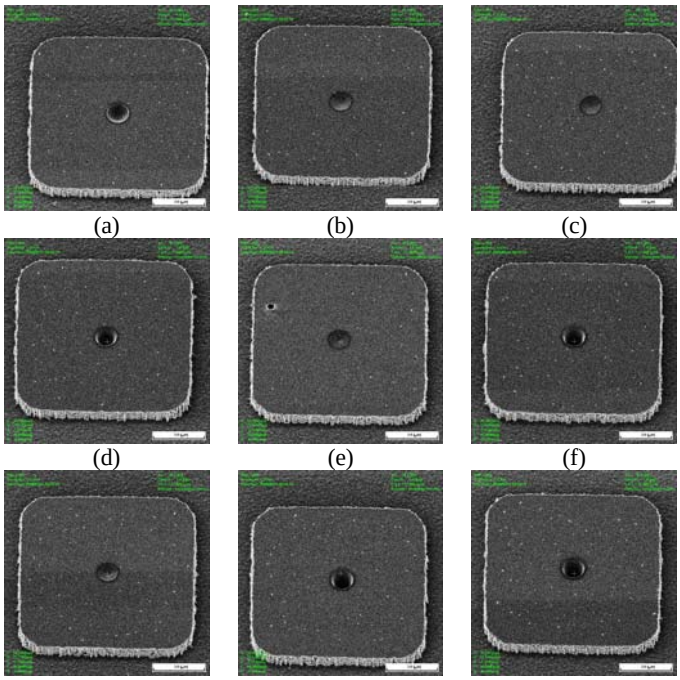

(a) (b) (c)

(d) (e) (f)

(g) (h) (i)

Fig. 4. FIB fabricated circular cone to the orthogonal array.

3. Experimental result

Table 3 Evaluation form based on the defined feature

	Structure dimension				Efficiency		
No	Width (nm)	Height (nm)	Side wall angle (degree)	physical error (nm)	Sputter yield (nm^2/pC)	Time	Cost (200EA, Won)
1	1238.5	459.5	33.6	10.8	1432926.0	11	876973
2	1199.5	205.7	18.8	6.1	1654608.0	4	759477
3	1215.0	170.0	15.7	4.8	1871086.4	3	671608
4	1195.5	735.1	50.9	16.7	1468597.9	16	855671
5	1223.0	148.7	13.6	6.0	2486783.7	2	505326
6	1179.5	768.6	54.3	30.3	629341.7	38	1996748
7	1125.0	231.8	21.8	8.8	1640149.9	4	766172
8	1172.0	769.7	52.9	27.2	762776.5	31	1647451
9	1183.5	769.9	53.3	27.3	861307.9	28	1458987
Ref. condition	1200.0	600.0	45.0	0.0	lager	smaller	smaller

Table 4 SN ratio of estimation result

	Structure dimension				Efficiency		
No	Width (nm)	Height (nm)	Side wall angle (degree)	physical error (nm)	Sputter yield (nm^2/pC)	Time	Cost (200EA, Won)
1	-31.7	-43.0	-21.2	-20.7	123.1	-20.8	-118.9
2	6.0	-51.9	-28.4	-15.7	124.4	-12.0	-117.6
3	-23.5	-52.7	-29.3	-13.5	125.4	-9.5	-116.5
4	-13.1	-42.6	-15.4	-24.5	123.3	-24.1	-118.6
5	-27.2	-53.1	-29.9	-15.5	127.9	-6.0	-114.1
6	-26.2	-44.5	-19.4	-29.6	116.0	-31.6	-126.0
7	-37.5	-51.3	-27.3	-18.9	124.3	-12.0	-117.7
8	-28.9	-44.6	-17.9	-28.7	117.6	-29.8	-124.3
9	-24.3	-44.6	-18.4	-28.7	118.7	-28.9	-123.3

3.1 Evaluation

In order to evaluate the sputtering characteristics, when fabricating the microscale mold, the feature definition, as shown in Fig. 5, was introduced. From this definition, the structural stability (diameter, depth, sidewall angle), inevitable physical phenomenon, and efficiency (sputter yield, cost) were evaluated. Furthermore, some physical phenomena influenced by processing parameters were investigated.

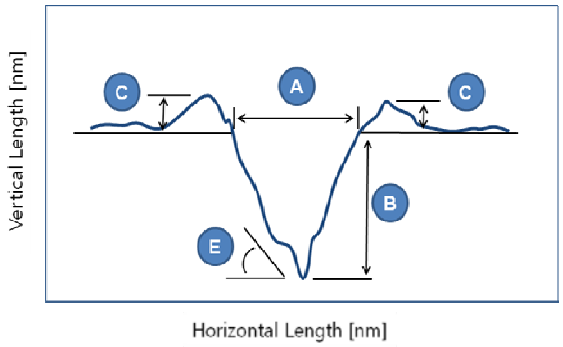

Fig. 5 Feature definition of evaluation for FIB sputtered structure for microscale mold application: width (A), depth (B), edge of the rim (C), and sidewall angle (E).

3.2 Experimental results

From AFM measurement, width (A), depth (B), edge of the rim (C), and sidewall angle (E) were measured as shown in Table 3. Based on Table 3, the sputter yield and cost were evaluated. For cost analysis, total production and cost per hour are 100 each and 200 dollars respectively. The robust design of Taguchi method use signal-to-noise (S-N) ratio by reducing the noise factor in order to evaluate the result adequately. SN ratio is the ratio of input signal and noise factor.

SN ratio is the objective function which is different to character of quality. In this research, SN ratio function (Eq. (1)) is to be small a expectation loss ($L(y)=kE(1/y^2)$) in lager the better characteristic.

On the contrary, smaller better characteristic is the best case as decreasing character to analyze and that equation is like Eq. (2).

In this study, lager the better characteristic was used to evaluate the sputter yield and smaller the better characteristic was applied to evaluate A, B, C, E and cost.

$$SN = -10\log[\frac{1}{n}\sum_{i=1}^{n}\frac{1}{y_i^{\,2}}] \quad (1)$$

$$SN = -10\log[\frac{1}{n}\sum_{i=1}^{n}y_i^{\,2}] \quad (2)$$

In Eq. (1-2), n represents the measured value, and y_i represents the measured characteristic value.

Table 5 Response table for SN ratio of width

Factor	Effect (dB)			Deviation	PC (%)
	1	2	3		
A	-16.4	-22.2	-30.3	13.9	26.6
B	-27.4	-16.7	-24.7	10.7	20.6
C	-29.0	-10.5	-29.4	19.0	36.4
D	-27.8	-19.2	-21.8	8.5	16.4

Table 6 Response table for SN ratio of height

Factor	Effect (dB)			Deviation	PC (%)
	1	2	3		
A	-49.2	-46.7	-46.8	2.4	15.9
B	-45.6	-49.9	-47.3	4.2	27.8
C	-44.0	-46.4	-52.4	8.3	54.6
D	-46.9	-49.3	-46.6	0.3	1.7

Table 7 Response table for SN ratio of side wall angle

Factor	Effect (dB)			Deviation	PC (%)
	1	2	3		
A	-26.3	-21.6	-21.2	5.1	22.4
B	-21.3	-25.4	-22.4	4.1	18.1
C	-19.5	-20.7	-28.9	9.4	41.3
D	-23.2	-25.0	-20.9	4.1	18.2

Table 8 Response table for SN ratio of physical error

Factor	Effect (dB)			Deviation	PC (%)
	1	2	3		
A	-16.6	-23.2	-25.4	8.8	36.7
B	-21.3	-20.0	-24.0	4.0	16.6
C	-26.3	-23.0	-16.0	10.4	43.2
D	-21.6	-21.4	-22.2	0.8	3.4

Table 9 Response table for SN ratio of sputter yield

Factor	Effect (dB)			Deviation	PC (%)
	1	2	3		
A	124.3	122.4	120.2	4.1	26.5
B	123.6	123.3	120.0	3.3	21.2
C	118.9	122.1	125.9	7.0	45.1
D	123.2	121.5	122.1	1.1	7.2

Table 10 Response table for SN ratio of cost

Factor	Effect (dB)			Deviation	PC (%)
	1	2	3		
A	-117.7	-119.6	-121.8	4.1	26.1
B	-118.4	-118.7	-121.9	3.5	22.6
C	-123.1	-119.8	-116.1	7.0	44.3
D	-118.74	120.43	-119.84	1.10	7.03

Using Eq. (1-2), the measured data in Table 3 converted into SN ratio in Table 4. On the basis of this SN ratio, influences to each experimental factor ware calculated in Table 5-10. Deviations in all tables are defined as the difference between maximum and minimum values of level effect of factors.

Percentage contribution represents a percentage of ratios of each factors to the total sum of deviation difference. A, B, C, and D represent total count, dwell time, overlap, and number of slice, respectively.

The result of Table 4-10 was represented in Fig. 6. The higher SN ratio is, the better experimental condition or reference value of evaluation represents.

For the analysis of structural stability, the optimum experimental condition from Table 5-6 was deduced. There are 3 kinds of factors, including width, depth, and sidewall angle, for structural stability. Each factor gives differenent optimum conditions. However, the width variation is smaller than any other factor. Based on this result, both depth and height were considered to find out the optimum condition. For both factors, they give almost similar experimental condition. Because the SN ratio of A2 and A3 in Table 6 shows small difference, A3 in Table 3 was adopted by considering the sidewall angle as the optimum condition.

In case of physical phenomena (surface amorphization), optimum conditions were like Table 8.The optimum conditions of the sputter yield and cost analysis were same (Table 9-10).

Except for volume optimization, which is the same as structural stability, the optimal condition for the physical error, sputter yield, and cost gave very short fabrication time, which are 2 and 1 second respectively. It indicates that the physical error (edge of the rim) accumulates as a function of ion beam irradiated time. In case of the cost, it is related to the sputter yield. Thus, the reason why short fabrication is occurred is that the sputter yield is continuously decreasing tendency before reaching at a specific saturation point.

Table 11 Optimal condition

Evaluation value	Optimal condition			
	Total count	Dwell time	Overlap	No. of slice
Width	10000	1	1	10
Height	20000	0.5	0.5	15
Side wall angle	30000	0.5	0.5	15
Physical error	10000	1	0.5	10
Sputter yield	10000	0.5	1.5	5
Cost	10000	0.5	1.5	5

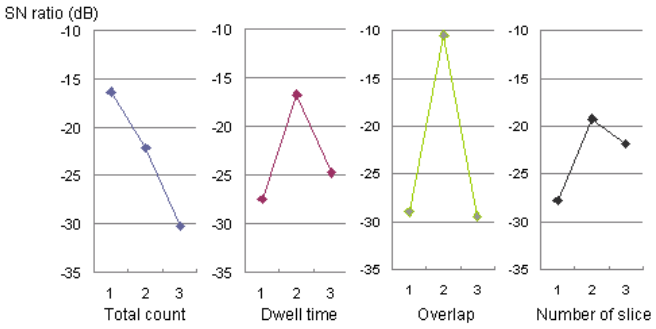

(a) Width

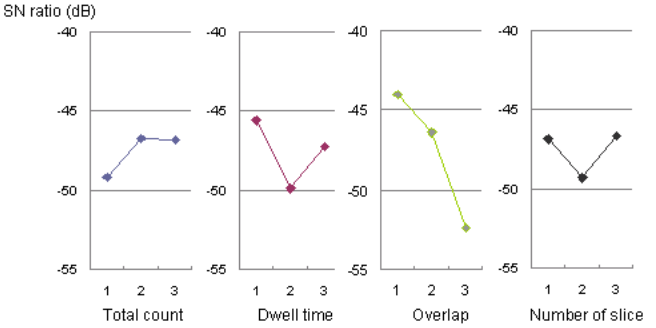

(b) Depth

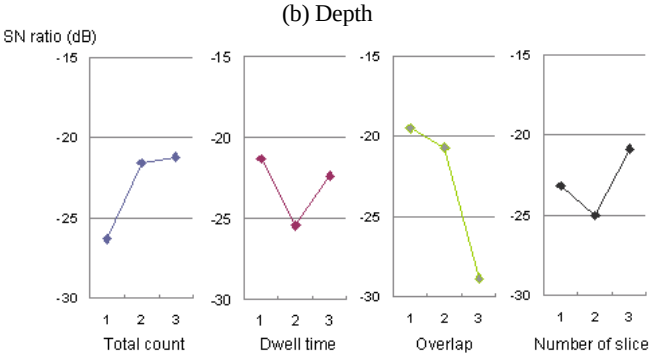

(c) Side wall angle

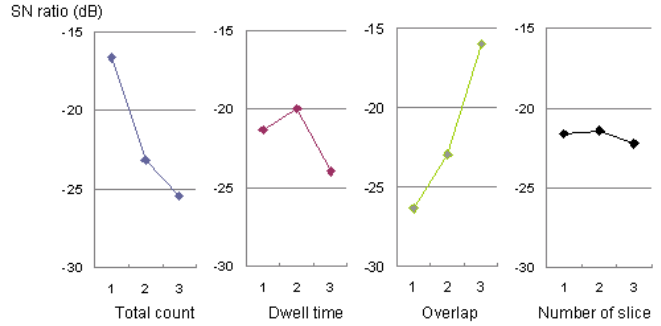

(d) Physical error

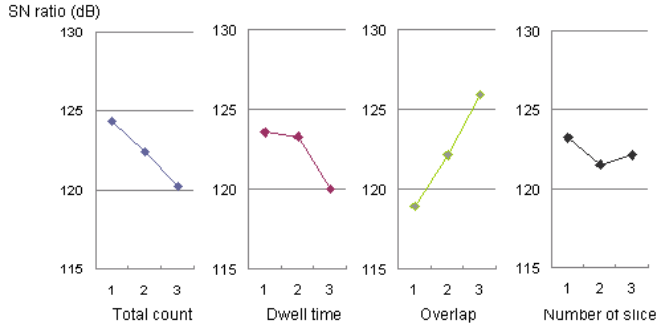

(e) Sputter yield

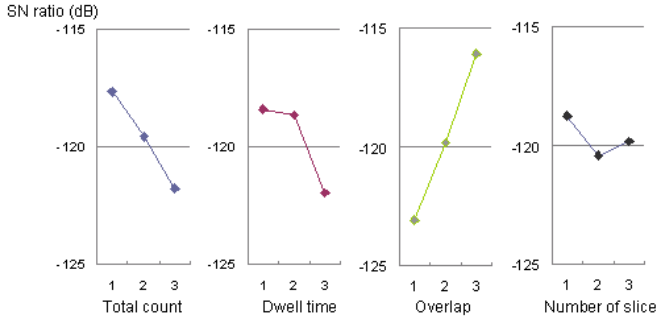

(f) Cost

Fig. 6 Variation graph of SN ratio about the evaluation values

3.3 Polymer replication

Using the optimal condition for structural stability, a silicon mold having conical shape for replicating both PDMS and PUA, which were specially offered by Nano fusion laboratory in Seoul National University (SNU), was prepared, as shown in Fig. 7-8.

4. Conclusions

Experiments which know effects of fabrication conditions about focused ion beam were performed using Taguchi method. Cones which have micro-nano scales were fabricated to silicon wafer. Structure stability, physical phenomenon, sputter yield and cost of cones were evaluated respectively and then, optimum fabrication conditions could be searched as SN ratio.

To evaluate structure stability, width, depth and sidewall angle of cone were estimated using AFM. Width of cone is very similar to width of shape to plan in all experiments and then, optimum conditions about depth and side wall angle of shape were analyzed. Other fabrication conditions except of condition of total count were same about depth and side wall angle but 30000 was adopted about optimum condition of total count relate to structure stability. Because Value of SN ratio at fabrication condition about each total count (20000, 30000) is almost same.

Optimum fabrication conditions were analyzed about physical phenomenon, sputter yield and cost. But those optimum conditions weren't important to fabricate cone shapes because fabrication time is very small at those optimum fabrication conditions. In shortly, if fabrication time is smaller and smaller, sputter yield can be increased and physical phenomenon can be decreased. This is that focused ion beam fabrication absolutely had the case of phenomenon. Moreover SN ratio variation of sputter yield was similar to SN ratio variation of cost.

In future, dimensions of cone shape which was fabricated at optimal fabrication condition will be estimated and analyzed. Therefore fabrication improvement of optimum condition will be searched.

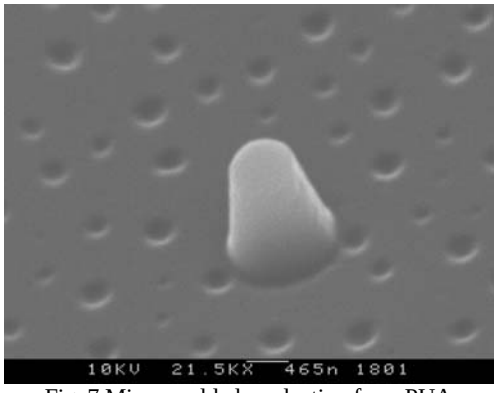

Fig. 7 Micro-molded production from PUA

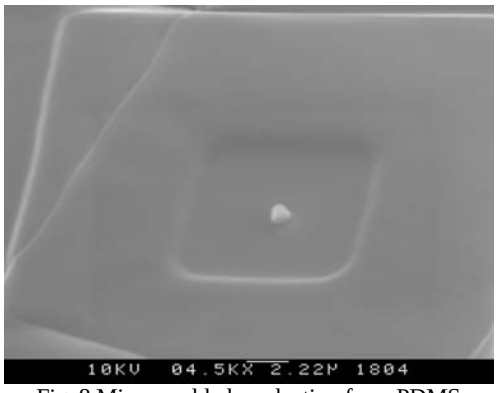

Fig. 8 Micro-molded production from PDMS

ACKNOWLEDGEMENT

This project is conducted through the Practical Application Project of Advanced Microsystems Packaging Program of Seoul Technopark (No. 10029790) and the Grant-in-Aid for Next-Generation New Technology Development Programs (No. 10030046), funded by the Ministry of Commerce, Industry and Energy. And it is also funded by the Engineering Research Institute, the ERC (Micro-Thermal System Research Center).

REFERENCES

1. A. A. Tseng, "Recent Developments in Nanofabrication using Focused Ion Beams," Small, Vol. 1, pp. 924-939, 2005.
2. S. Reyntjens and R. Puers, "A review of focused ion beam applications in microsystem technology," J. Micromech. Microeng., Vol. 11, pp. 287-300, 2001.
3. M. Sugiyama and G. Sigesato, "A review of focused ion beam technology and its applications in transmission electron microscopy," Journal of Electron Microscopy, Vol. 53, pp. 527-536, 2004.
4. S.W. Youn, C. Okuyama, M. Takahashi, and R. Maeda, "A study on fabrication of silicon mold for polymer hot-embossing using focused ion beam milling," Journal of Materials Processing Technology, Vol. 201, pp. 548-553, 2008.
5. H.W. Sun, J.Q. Liu, D. Chen, and P. Gu, "Optimization and experimentation of nanoimprint lithography based on FIB

fabricated stamp," Microelectronic Engineering, Vol. 82, pp. 175-179, 2005.
6. L.Y. Hong, D. H. Lee, and D. P. Kim, "Fabrication and application of novel hydrophilic nanomold," Journal of Physics and Chemistry of Solids, Vol. 69, pp. 1436, 2008.
7. M.J. Vasile, Z. Niu, R. Nassar, W. Zhang, and S. Liu, "Focused ion beam milling: Depth control for three-dimensional microfabrication," J. Vac. Sci. Technol. B, Vol. 15, pp. 2350-2354, 1997.
8. D.P. Adams, M.J. Vasile, and T. M. Mayer, "Focused ion beam sculpting curved shape cavities in crystalline and amorphous targets," J. Vac. Sci. Technol. B, Vol. 24, pp. 1766-1775, 2006.
9. D.P. Adams and M. J. Vasile, "Accurate focused ion beam sculpting of silicon using a variable pixel dwell time approach," J. Vac. Sci. Technol. B, Vol. 24, pp. 836-843, 2006.
10. R. Nassar, M.J. Vasile, and W. Zhang, "Mathematical modeling of focused ion beam microfabrication," J. Vac. Sci. Technol. B, Vol. 16, pp. 109-115, 1997.
11. Y. Fu and N. K. A. Bryan, "Fabrication of three-dimensional microstructures by two-dimensional slice by slice approaching via focused ion beam milling," J. Vac. Sci. Technol. B, Vol. 22, pp. 1672-1678, 2004.
12. W.C.L. Hopman, F. Ay, W. Hu, W.J. Gadgil, L. Kuipers, M. Pollnau, and R. M. Ridder, "Focused ion beam scan routine, dwell time and dose optimizations for submicrometre period planar photonic crystal components and stamps in silicon," Nanotechnology, Vol. 18, pp. 195305, 2007.